Revista de Ciencias Agrícolas
e-ISSN 2256-2273
https://doi.org/10.22267/rcia.20244102.3237

Research article: Forestry.

Net primary productivity in a Tropical Dry Forest of northern Colombia

Productividad primaria neta en un Bosque Seco Tropical del norte de Colombia

Sonia Esperanza Aguirre-Forero[1*]; Arturo Rozo-Celemín[2]; Nelson Virgilio Piraneque-Gambasica[3]

Authors Data

1. Professor, Ph., Universidad del Magdalena, Santa Marta, Colombia, saguirre@unimagdalena.edu.co, https://orcid.org/0000-0002-6975-1940
2. Student, M.Sc., Escuela Naval de Cadetes, Santa Marta, Colombia artur29ias@gmail.com, https://orcid.org/0000-0003-3394-3198
3. Professor, Ph., Universidad del Magdalena, Santa Marta, Colombia, npiraneque@unimagdalena.edu.co, https://orcid.org/0000-0002-4264-9428

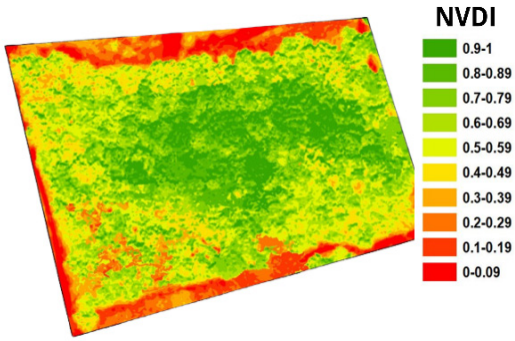

Cite: Aguirre-Forero, S.E.; Rozo-Celemín, A.; Piraneque-Gambasica, N.V. (2024). Net primary productivity of photosynthetic plants in Tropical Dry Forest of northern Colombia. *Revista de Ciencias Agrícolas.* 41(3): e3237. http://doi.org/10.22267/rcia.20244103.237

Received: January 22 2024 Accepted: October 10 2024

ABSTRACT

Tropical dry forests are the world's second most relevant forest type, home to unique vegetation and highly threatened by human activity. This study aimed to determine changes in plant biomass within a tree-hectare permanent plot of tropical dry forest (TDF) at the Universidad del Magdalena over 12 months. The composition, structure, and plant dynamics were characterized using drone imagery and allometric equations for dry climates. Biomass was calculated for 848 trees and shrubs with a diameter at breast height (DBH) over 10 cm, and a Normalized Difference Vegetation Index (NDVI) time series was established. It was possible to identify the change in NDVI with a positive trend in areas with higher soil moisture, higher coverage, vegetation network, and limited access. Likewise, the findings show that areas with lower coverage have greater accessibility and lower diversity. The vegetation cover dynamics within the Universidad del Magdalena's TDF plot revealed low variability in NDVI over the study period, with values exceeding 0.7 in 58% of observations, reflecting a linear trend with the rainy seasons. Estimating the vegetal cover biomass is feasible using differentiated indices and techniques that reduce costs and time and do not have destructive implications for the vegetation.

Keywords: allometric equations; Colombian Caribbean; drought; plant cover; rain; vegetation.

RESUMEN

Los bosques secos tropicales (BsT) son el segundo tipo de bosque más importante del mundo, albergan una vegetación única y están amenazados por la actividad humana. Este estudio tuvo como objetivo determinar los cambios en la biomasa vegetal en una parcela permanente de tres ha de BsT en la Universidad del Magdalena durante 12 meses. Se caracterizó la composición, estructura y dinámica vegetal utilizando imágenes de drones y ecuaciones alométricas para climas secos. Se calculó la biomasa de 848 árboles y arbustos con diámetro a la altura del pecho (DAP) mayor a 10 cm y se estableció una serie temporal del Índice de Vegetación de Diferencia Normalizada (NDVI). Fue posible identificar el cambio en el NDVI con una tendencia positiva en áreas con mayor humedad del suelo, mayor cobertura, red de vegetación y acceso limitado. Asimismo, los hallazgos muestran que las áreas con menor cobertura tienen mayor accesibilidad y menor diversidad. La dinámica de la cobertura vegetal en la parcela de BsT de la Universidad del Magdalena reveló baja variación en NDVI en el periodo de estudio, con valores superiores a 0,7 en el 58% de las observaciones, reflejando tendencia lineal con las épocas lluviosas. La estimación de la biomasa de la cobertura vegetal es factible utilizando índices diferenciados, lo que reduce costos y tiempo sin implicaciones destructivas para la vegetación.

Palabras clave: ecuaciones alométricas; Caribe colombiano; cobertura vegetal; lluvia; sequía; vegetación.

INTRODUCTION

Forests cover 1/3 of the earth's surface. Of these, Tropical Dry Forests (TDF) are the second most crucial forest type, covering about 42% of the tropical and subtropical forest area (Hasnat & Hossain, 2020). Almost 50% of the TDF are found in the Americas and are the most threatened of all forest types due to climate change and anthropogenic intervention, manifested in logging, agricultural frontier expansion, forest fires, and change of use. Despite this, there are few studies on the potential of TDF to produce biomass and serve as a carbon sink (Gwal *et al*., 2020; Thakur *et al*., 2019) in the conditions of northern Colombia, so it is necessary to deepen and link research on the subject. In the Caribbean region, the largest and best-conserved areas of TDF are located in the coastal zone, specifically in areas adjacent to Santa Marta city, the foothills of the northern flank of the Sierra Nevada de Santa Marta, and the south of La Guajira, in the vicinity of the Tayrona National Natural Park. On the grounds of the University of Magdalena, there is a permanent plot (relic) of TDF, a strategic ecosystem for long-term research development, to broaden knowledge and appreciate fundamental contributions to mitigating climate change and reducing the pressure of human activities (Mngadi *et al*., 2022).

Indeed, in ecosystems, producing organic materials (biomass) and their decomposition stabilizes biogeochemical cycles (Thakur *et al*., 2019), including carbon, which is essential for soil conservation. The biomass's quantity and quality reflect the system's state. They are parameters for estimating CO2 sinks, quantifying plant nutrients, determining primary photosynthetic productivity (PPN), and comparing species and vegetation types at different sites (Anaya-Acevedo *et al*., 2008).

Biomass in tropical dry forests retains the majority of global terrestrial carbon. It undertakes a vital role in effecting the preservation of biodiversity, with high species diversity driven by local conditions, including low humidity and nutrient-poor soils. Biomass, which includes live and dead plant material, provides essential habitats and vital nutrients for a wide range of species, resulting in the protection of biodiversity resources necessary to restore disturbance equilibria across both natural and caused ecological damages (Stan & Sanchez-Azofeifa, 2019; Siyum, 2020).

As can be verified, aboveground biomass is mainly linked to leaves and stems; it is directly counted in grams by destructive methods (Schlegel *et al*., 2001), but in large areas and protected or vulnerable ecosystems, it is not feasible. An alternative is the use of vegetation indices obtained by remote sensing that captures multispectral images from satellites or unmanned aerial vehicles (drones) - MODIS, taking advantage of the relationship between vegetation cover, a fraction of photosynthetically active radiation absorbed, and the Normalized Green Index (NDVI) (Thakur *et al*., 2019; Anaya-Acevedo *et al*., 2008); This has facilitated the use of NDVI as an indicator of net photosynthetic productivity (biomass) at the landscape scale (Zaitunah *et al*., 2018) and its application in remote sensing for vegetation cover based on the product of the relationship between solar radiation and canopy, which is summarized as the contrast between the red band of the visible spectrum (645 nm) and the near-infrared (700-1300 nm) because leaf pigments offer low reflectivity in the red band and high reflectivity in the near-infrared (Anaya-Acevedo *et al*., 2008; Guzmán Q. *et al*., 2019).

Similarly, allometric equations can be used from direct measurements (Gómez *et al*., 2021), wherein forestry, height, diameter at breast height, and wood density are the variables to be measured to calculate biomass as the dependent variable. Height and diameter are easily measured in the field, while density is obtained in the laboratory from small wood samples. However, according to Anaya-Acevedo *et al*. (2008), allometric equations reported in the literature show that information for many species is scarce (Gómez *et al*., 2021), and the behavior of biomass is not linear as a function of individual diameter and stand diameter frequencies. These considerations are interesting when establishing the relationship between biomass and remotely sensed data (Srinivas & Sundarapandian, 2019). At the same time, multispectral sensors on drones allow direct and continuous observation of the variables that characterize the forest surface; they provide data in real-time and in a scalable manner; they are an efficient tool for recognizing and spatially monitoring the territory, identifying spatial patterns and anomalies, as well as locating, delimiting, and measuring their evolution over some time (Baseca, 2019).

In addition, the Normalized Green Index from Rouse Jr. *et al*. (1974), known as NDVI, derived by the equation NDVI = (NIR - RED)/(NIR + RED), from MOD09GQ (TERRA AM) and MYD09GQ (AQUA PM) surface reflectance data from the MODIS (Moderate Resolution Imaging Spectroradiometer) sensor is a widely used variable, with values

ranging from -1. 0 and 1.0 (NDVI), and its products have a daily temporal resolution and a spatial resolution of 250m x 250m (Becker-Reshef *et al*., 2010). This index has been prioritized in various research studies for vegetation cover and endorsed as an indicator of vegetation cover by different institutes.

It is estimated that 90% of the TDF in the Colombian Caribbean has been lost, and if we add that it is a complex ecosystem with high deterioration, fragmentation, and vulnerability to land use change, monitoring its dynamics allows us to learn more about its close interrelationships and the benefits it provides at an economic, social and environmental level, such as CO_2 sequestration, soil protection against erosion, storage, and regulation of rainwater, nutrient cycling, production of fruit and leaf litter for the food chain, absorption and transformation of thermal and light energy, and also as a genetic laboratory to tolerate extreme events, the basis for buffering and mitigating the so-called climate change phenomenon in the future.

Therefore, it was proposed to estimate the foliar PPN of the permanent plot of relicts of Tropical Dry Forest (TDF) located at the University of Magdalena, using unmanned aircraft and five allometric equations developed for dry tropical climates, based on the diameter at breast height (DBH) of 10 cm per individual and drone images obtained between July 2020 and August 2021, to estimate and analyze the tree biomass of the system, information that will contribute to understanding the dynamics of the vegetation cover in conditions of the Colombian Caribbean, where unfortunately a loss of more than 90% of the TDF is estimated (Benítez *et al*., 2014).

MATERIAL AND METHODS

In the first phase, an approach to the quantification of biomass was carried out through the capture of images by drone to establish the Normalized Green Index (NDVI); the second phase determined allometric equations based on the diameter at breast height (DBH) of 10 cm per individual, for which a species inventory was necessary to estimate the tree biomass of the campus.

Location and description of the study area. Magdalena Department, Santa Marta, Colombia, Campus of the University of Magdalena. Centro de Desarrollo Agrícola y Forestal (CDAF) coordinates 74°07’ 0” and 74°12’0” W 11°11’ 0.9” and 11°13’ 29.6” N, and 74°11’0” W in the city of Santa Marta (Figure 1). Average temperature of 29.5°C, average annual rainfall of 700 mm, relative humidity of 70%, altitude of ten m.a.s.l., influenced by the trade winds from the northern hemisphere, semi-arid climate with a marked water deficit in the dry season, with megathermal environments and plant formations classified as Sub-Xerophytic Zonobiomes according to Rangel *et al*. (2009). Annual potential evapotranspiration (ETP) or reference evapotranspiration (ETo) fluctuates between 1300 and 1412 mm (Revueltas *et al*., 2020), and relative humidity is between 65% and 80% (Girón-Angarita, 2021).

Left: Permanent relict plot of Tropical Dry Forest (TDF) Universidad del Magdalena. **Right**: TDF relict flight plan - Granja Experimental Universidad del Magdalena.

Figure 1. Location of the study area.

The area's topography is flat, with soils with a texture varying from loam to clay-sandy loam, low organic matter content, and the presence of salts. Soils have developed on a terrace plane from quaternary alluvial deposits, constituting the parental material classified in the order Entisols and suborder Psamments (Aguirre *et al*., 2022), characterized by being poorly evolved, with a predominance of coarse textures, subangular block-type structures in the epipedons, and without structure in the endopedons. Chemically, soils with neutral to alkaline pH, high Na, Ca, Mg, and K concentrations, low CO contents, and a cation exchange capacity (CEC) value between 10-20 cmol+ kg^{-1} (Girón-Angarita, 2021).

The Centre for Agricultural and Forestry Development (CDAF) has an area of 24 hectares (ha), which are distributed as follows: 3.0 ha of tropical dry forest in recovery; 12.72 ha in fallow; 0.76 ha occupied by artificial ponds for research and fish production purposes; and 5.91 ha between transitory and perennial crops. The permanent TDF relict plot was defined 12 years ago and complied with the specifications of this TDF system as stipulated by the Alexander Humboldt Research Institute. The activities were carried out in two phases: Phase I focused on NDVI estimation using drone imagery, and Phase II involved species identification, biometric measurements, and biomass estimation using allometric equations tailored to tropical dry climates.

Phase I. Delimitation of the study area: the university property (Arboletes and TDF's permanent plot) was considered for programming monthly flight plans with the free Android application Pix4Capture, designing routes in the form of transects for the photogrammetric survey of the area. Figure 1 right defined the polygon to be overflown and the flight parameters (speed, camera tilt, and overlap), with an approximate flight time of 22 minutes.

Image processing. Using the Pix4Mapper program, images were scaled for grid construction, calibration, and densification of point clouds to obtain orthomosaics and digital surface models (DSM) of the study area.

In the calculation of the Normalized Difference Vegetation Index (NDVI), the presence of vegetation in the area and its activity were assessed and related to photosynthetic activity, so reflectance values corresponding to the different wavelengths were used (Gautam *et al*., 2019; Singh *et al*., 2020), where the values of this index are within the interval (-1,1), equation 1.

$$NDVI = \frac{NIR - R}{NIR + R} \quad (1)$$

Phase II. The census of individuals and identification of tree species were carried out through the photographic registration of the stem, leaves, fruits, and flowers of each individual based on the attributes described in the Herbarium of the University of Magdalena and the Catalogue of Plants and Lichens of Colombia's Institute of Natural Sciences of the National University of Colombia (Bernal *et al*., 2020).

The biometric measurements of individuals with DBH > 10 cm were carried out following the methodological and operational guidelines established in the National Forest Inventory Field Manual (IDEAM, 2018). Each individual's stem's perimeter was recorded at 1.30 m from the soil to estimate the diameter at breast height (DBH) for subsequent conversion to diameter according to D=P/π, where D is the diameter and P is the perimeter measured. For multi-stemmed individuals, the root mean square diameter (RMD) was calculated using equation 2:

$$RMD = \sqrt{\sum_{i=1}^{n} DBH_i^2} \quad (2)$$

The total height of each individual was estimated using a clinometer whose operation is based on trigonometric principles that consider the horizontal distance and the angle formed between the individual's base and the apex, expressed as equation 3:

$$H = X * (tan\ \beta\ -\ tan\ tan\ \theta\ ) \quad (3)$$

Where H is the total height, X is the horizontal distance from the base of the individual to the observation point, θ is the angle formed between the horizontal axis and the individual's bottom, and β is the angle formed between the horizontal axis and the

apex of the individual. The allometric equations selected for biomass estimation are presented in Table 1, which were developed for dry tropical climates by Chave *et al*. (2001), Phillips *et al*. (2011), and Alvarez *et al*. (2012) to estimate aboveground biomass in natural forests in Colombia. They correspond to three input models, which consider total height (H), stem diameter (D), and stem density (ρ).

Table 1. Allometric equations for estimating tree biomass in dry tropical climates.

		Equations	Source
1.	***a***	$BA = 0.112(\rho D^2 H)^{0.916}$	(Chave *et al*., 2001)
2.	***b***	$ln\ (BA)\ = -2.29 + 0.932\ ln(D^2 H\rho)$	(Phillips *et al*., 2011)
3.	***c***	$ln\ (BA)\ = -2.825 +\ ln(D^2 H\rho)$	
4.	***d***	$ln\ (BA)\ = -2.328 + 0.937\ ln(D^2 H\rho)$	(Alvarez *et al*., 2012)
5.	***e***	$ln\ (BA)\ = -2.27 + 2.081\ ln(D) + 0.587\ ln(H) + 1.092\ ln(\rho)$	

ρ= wood density, D=D =D= diameter at breast height, H=H =H= tree height

Statistical analysis. With exploratory analysis of the NDVI time series, we searched for outliers (with the criterion of 3 standard deviations) to consecutively estimate the time trend using Spearman's correlation test as a function of time with a degree of significance, which was verified using the p-value associated with Spearman's statistic, allowing to analyze the vegetation dynamics in terms of increase (positive correlation) and decrease (negative correlation). Spearman's test allowed for the detection of the temporal trend in the NDVI series but did not identify the factors involved. To determine the control exerted by climate on plant activity and to isolate it from other factors, a multivariate regression of mean NDVI values against climatic variables was performed for each cover. As an intermediate step, a correlation analysis was carried out to select the most appropriate climatic time series.

For the March and August images, it was found that the climatic time series with the highest correlation with NDVI was the three months before each image's acquisition date, which was used as covariates in the regression analysis. Two other covariates, Julian day and year of image acquisition, were also introduced, as these could affect NDVI. To determine the variables that significantly explain the temporal evolution of NDVI over each cover, a stepwise regression procedure based on AIC (Akaike's information criterion statistic), implemented in R statistical software (R Core Team, 2022), was used. For spatial analysis, the multivariate regression was repeated pixel by pixel only in areas at risk of erosion (without vegetation); this allowed us to obtain a spatially distributed map of NDVI trends that were not explained by climatic variables and thus to identify areas experiencing vegetation degradation or recovery processes. A correlation analysis between NDVI evolution

and topographic factors (altitude, slope, and potential incoming solar radiation), a bootstrap procedure to determine the correlation's statistical significance, and finally, an NDVI image series principal component analysis was performed to explain the spatiotemporal data variability.

RESULTS AND DISCUSSION

Phase I. Negative values represent bare and artificial soils, 0-0.33 for water-stressed or diseased plants, 0.33-0.66 for moderate water stress, and 0.66-1 for healthy plants (Figure 2).

Figure 2A shows NDVI from August 2020 calculated from ortho mosaics of multispectral images captured with 42 flight campaigns. Previously, at the beginning, it was confirmed that artificial cover (non-vegetation) and water bodies had values close to 0. In contrast, low or pruned grasses had values between 0.3 and 0.5, and secondary vegetation (shrubs and ornamentals) values were between 0.5 and 0.6. On the other hand, tall and vigorous vegetation (trees and shrubs) presented higher values, close to 0.7.

The estimated indices between September 2020 and July 2021 show NDVI values ≥ 0.7 in more than 15% of the total study area (35240.33 m^2). However, from January to May 2021, the areas of NDVI ≥ 0.7 were less than 15%. Between June and July, the area was observed to decrease to 10%, which coincided with a period of high solar intensity and low precipitation. Between November and December 2020, NDVI values ranged between 0.8 and 1, reaching maximum values and an area of 37.34% and 35.3%, respectively (Figure 2B). Meanwhile, NDVI values ≤ 0.3 are maintained in the other months of 2021 below 10%, accentuated in northern and south-western areas where there is road access and some stubble. NDVI values between 0.3 and 0.69 correspond to grassland and low vegetation (Figure 2C).

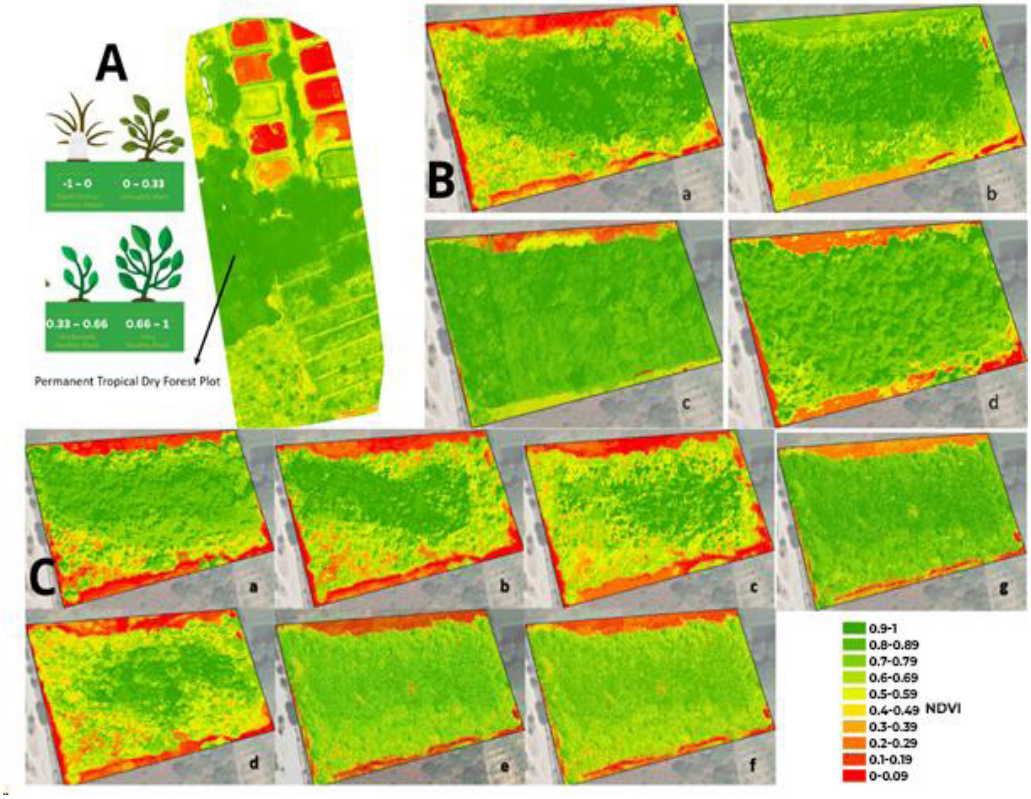

Figure 2. NDVI spatial distribution in the years 2020 and 2021, calculated from orthomosaics of multispectral images. **A)** NDVI in August 2020. **B)** NDVI spatial distribution in a) September, b) October, c) November, and December of 2020. **C)** NDVI spatial distribution of a) January, b) February, c) March, d) April, e) May, f) June, and g) July in 2021.

The range of NDVI variation in the study area was generally low. The fits obtained between NDVI and precipitation from the spatial point of view are acceptable for the study period, showing linear reciprocity between the months with the lowest rainfall and the lowest NDVI values. However, the change in biomass volume is not immediate; several variables must be evaluated as they are associated, for example, radiation, soil water balances, and nutrient effects that depend on the physical, chemical, and biological properties available, among others, that affect the growth of vegetation in terrestrial ecosystems (Paz Pellat & Díaz-Solís, 2018).

Remote sensing technology-enabled vegetation monitoring, growth, and development by applying empirical relationships calculated between vegetation biophysical variables.

NDVI's PCA image series allowed us to explain most spatiotemporal variability on a pixel-by-pixel basis by operating on the covariance matrix of the standardized data to construct orthogonal linear "Principal Components" (PC) combinations (López *et al*., 2020). The first principal component (CP1) contains most of the variance of the NDVI images; it best explains the spatiotemporal variability of NDVI in the TDF relict. Thus,

Figure 3 shows the first principal component (CP1) of the variability of the NDVI indices, which comprises 63.55% of the variance, showing in terms of units of variability (nodes) zones of red color with low variability (values close to zero), zones of high variability of blue color that correspond to the center of the relict (variability in the NDVI range ≥ 0.7), and zones of intermediate variability of yellow and green colors located at the relict boundary edges.

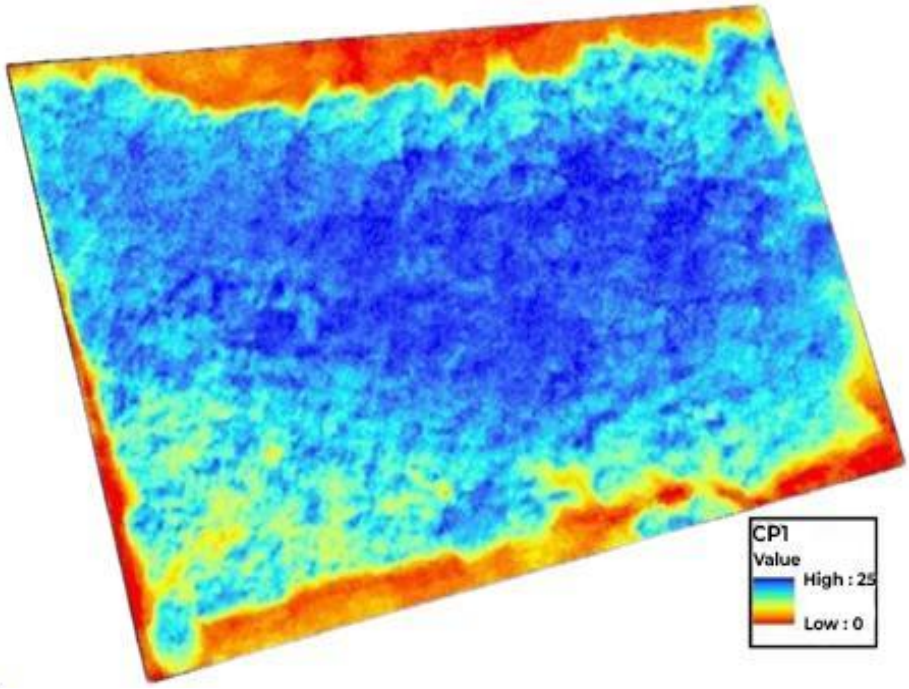

Figure 3. First Principal Component (CP1) of Normalized Difference Vegetation Index (NDVI) year 2021.

Monthly rainfall averages from the central synoptic station at Simón Bolívar Airport in Santa Marta in 2020 and 2021 show a close relationship between rainy seasons and increased vegetation indices in magnitude and extent (Figure 4). When plotting the chronological behavior of the vegetation indices and the climatic variables, a relationship was found between the average monthly rainfall data (bars) and the area percentages of the NDVI vegetation indices (lines), showing that in rainy periods (>1 mm/month), the NDVI indices greater than 0.79 (green) and the NDVI indices greater than 0.79 (green) increased in area (>30%). 79 (green color) and NDVI values lower than 0.5 reached area values close to 5%, while in the dry season (<1 mm/month), NDVI values higher than 0.79 showed a decrease with an area percentage lower than 20% (red colors).

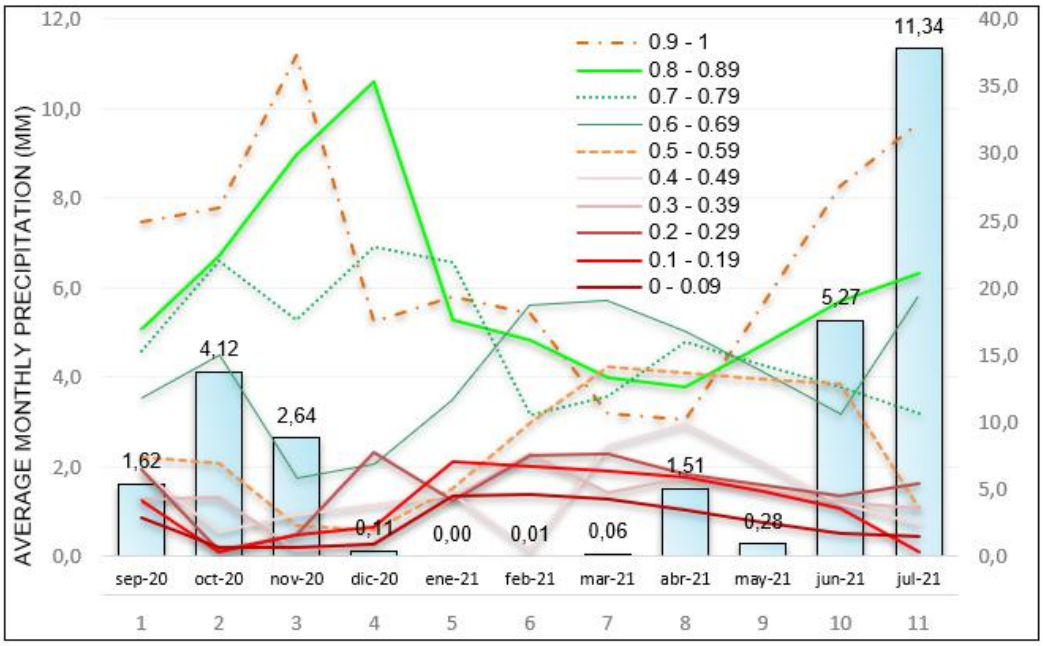

Figure 4. Percentage of area covered by NDVI (lines). Monthly average precipitation (bars).

Precisely for this short-term study (12 months), precipitation impacts the difference in biomass productivity (Table 2). These arguments contradict the evidence provided by Schlegel *et al*. (2001) when they show that climatic variables (temperature and precipitation) do not influence the vegetation cover index and that there is no correlation. They also mention that one of the direct causes of changes in land cover is deforestation, which is related to the expansion of cities and agriculture. Because of this, it is necessary to point out the specificity of time and climatic fluctuations of each study.

Table 2. Spatial and temporal variability of NDVI index, September 2020 - July 2021

NDVI	2020								2021													
	Sep.		Oct		Nov		Dec		January		February		March		April		May		June		July	
	m²	%	m²	%	m²	%	m²	%	m²	%	m²	%	m²	%	m²	%	m²	%	m²	%	m²	%
0.9 - 1	8780	24.92	9155.2	25.98	13157	37.34	6148	17.45	6806	19.31	6353	18.3	3736.5	10.6	3564	10.1	6596	18.72	9732	27.62	11388	32.3
0.8 - 0.89	5935	16.84	7890.7	22.39	10511	29.83	12440	35.30	6182	17.54	5666	16.8	4680.6	13.2	4432	12.6	5539	15.72	6683	18.96	7440	21.1
0.7 - 0.79	5361	15.21	7766.5	22.04	6199.	17.59	8109	23.01	7707	21.87	3713	10.5	4183.9	11.8	5614	15.9	5028	14.27	4425	12.56	3762	10.68
0.6 - 0.69	4141	11.75	5268.2	14.95	2054.1	5.83	2399	6.81	4088	11.60	6573	18.6	6715.	19.1	5876	16.7	4824	13.69	3735	10.60	6836	19.40
0.5 - 0.59	2595	7.36	2449.3	6.95	798.1	2.26	682.3	1.94	1773	5.03	3496	9.92	4951.4	14.	4802	13.6	4655	13.21	4504	12.78	1259	3.57
0.4 - 0.49	2213.	6.28	650.7	1.85	1082.9	3.07	1318	3.74	1637	4.65	167.3	0.47	2890.1	8.20	3451	9.79	2424	6.88	1362	3.86	863.6	2.45
0.3 - 0.39	1481	4.20	1557.4	4.42	129.2	0.37	341.5	0.97	1520	4.31	2683	7.62	1677.7	4.76	2064	5.86	1740	4.94	1409	4.00	1259	3.57
0.2 - 0.29	2262	6.42	164.7	0.47	557.9	1.58	2719	7.72	1458	4.14	2626	7.45	2675.5	7.59	2149	6.10	1878	5.33	1598	4.54	1893	5.37
0.1 - 0.19	1455	4.13	98.5	0.28	556.1	1.58	760.1	2.16	2465	7.00	2343	6.65	2236.3	6.35	2087	5.92	1684	4.78	1268	3.60	118	0.34
0 - 0.09	1009	2.86	236.1	0.67	235.2	0.67	317.9	0.90	1594	4.52	1613	4.58	1487.1	4.22	1194	3.39	898	2.55	590	1.67	519.9	1.48

Phase II. In the census of tree species on the university campus, 848 individuals with DBH>10 cm were identified and distributed among 31 species located as living fences, ornamentals, and fruit trees in the CDAF. There was a predominance for the species shown in Table 3.

Table 3. Species and their scientific names identified in the Universidad del Magdalena's tropical dry forest.

Specie (Scientific name)	%	Specie (Scientific name)	%
Tabebuia rosea	17.22	*Spondias mombin*	0.12
Azadirachta indica	13.92	*Enterolobium cyclocarpum*	14.39
Hura crepitans	8.96	*Prosopis juliflora*	9.79
Albizia niopoides	5.9	*Roystonea regia*	7.31
Mangifera indica	3.77	*Terminalia catappa*	5.19
Melicoccus bijugatus	2.12	*Samanea saman*	3.18
Platymiscium pinnatum	0.94	*Delonix regia*	1.53
Crescentia cujete	0.71	*Ficus benjamina*	0.83
Tamarindus indica	0.59	*Bulnesia arborea*	0.59
Sterculia apetala	0.35	*Livistona chinensis*	0.47
Cavanillesia platanifolia	0.24	*Ceiba pentandra*	0.35
Bursera simaruba	0.24	*Quadrella odoratissima*	0.24
Caesalpinia coriaria	0.12	*Guazuma ulmifolia*	0.24
Acrocomia aculeata	0.12	*Cecropia obtusifolia*	0.12
Ficus elastica	0.12	*Eriobotrya japonica*	0.12
Pseudobombax ellipticum	0.12	*Lonchocarpus Santae Martae*	0.12

Of the 31 species, 18 represent 97.5%, and the remaining 2.5% correspond to 13. *Tabebuia rosea* (17.22%), known in Colombia as Guayacan rosado, flormorado, ocobo, roble morado, roble rosado, cañaguate, and rosa morada, is a tree native to the tropophilous forests of the American intertropical zone that grows up to 30 meters. The

flower is pink and reaches up to 15 cm in length, and its fruits are narrow capsules that can contain between 200 and 300 flattened seeds (Pluemjit *et al*., 2018). Because of its size, it is used in agroforestry systems, shade, and decoration. It is used in traditional Thai medicine; its bark has antimicrobial, anti-inflammatory, antibacterial, antifungal, diuretic, and laxative properties (Sichaem *et al*., 2012).

Enterolobium cyclocarpum (14.39%), a tree native to the Americas in tropical and warm temperate regions, is one of the two species known as "elephant's ear", that reports nitrogen-fixing nodules in the roots that establish symbiosis with *Rhizobium*, which facilitates its adaptation and growth under conditions of high luminosity. White flowers with numerous stamens, tubular calyx, and corolla. Fruits with spiral-shaped pods (circular indehiscent) are woody, lustrous, light, or dark brown when ripe. Each fruit contains 10-15 seeds with ovoid, vino-tint-colored seeds and a pale line with the shape of the seed outline (oval shape).

Azadirachta indica (13.92%), also known as neem in Latin America, is a tree belonging to the Meliaceae family, native to India and Burma; it only lives in tropical and subtropical regions; it is a species with remarkable resistance to drought that typically survives in sub-arid conditions; and it reaches groundwater. Neem extracts act as an insecticide (Ochoa & Patricia, 2020). *Prosopis juliflora* (9.79%), a thorny tree native to the Caribbean known as Trupillo, a legume of dry, arid, and semi-arid zones in tropical and subtropical regions, reports association with nitrogen-fixing bacteria.

Hura crepitans (8.96%), also called catahoula, jabilla, ceiba amarilla, solimán, or salvadera, is a tree poisonous to humans from the Euphorbiaceae family. Because of its large size, it is an economically valuable timber species native to Central America. *Roystonea regia* (7.31%), known as royal palm, is an ornamental species native to southern Florida. *Albizia niopoides* (5.9%), a common native species in TDF belonging to the Fabaceae family (Bernal *et al*., 2020), is commonly used as wood for charcoal or barnyard posts.

Finally, *Terminalia catappa* (5.19%), a species widely distributed in Colombia with an origin under discussion, is a species that harbors a large fauna. Studies by Arrázola *et al*. (2008) [30] report that it is a high-protein and lipid-value kernel that can be used in animal feed due to its high capacity to adapt to diverse agroecological conditions. It should be noted that most of the vegetation obtained in this study is typical of the floristic composition of the Americas, specifically of the Caribbean region (TDF) (Benítez *et al*., 2014). Still, it is noteworthy that *Azadirachta indica* (13.92%), introduced to the campus in 2012 as a living fence, due to its adaptation, is surpassing the population species typical of the TDF, a condition for which it may be an invasive species [31] that breaks with the harmonious relationships with other local or native species, affecting the succession and landscape balance over time since the community structure and ecosystemic processes would be impacted, as stated by Mota *et al*. (2020).

Height. The distribution of total size (H) in the 12 most representative species is shown in Figure 5, where the values of Tabebuia rosea are in the extreme range between 3.1 and 17.2 m, with outliers reaching 19.6 m. *Enterolobium cyclocarpum* occurs between 3.2-20.8 m, with an outlier value of 23.2 m; *Azadirachta indica* between 4.1-10. 8 m; *Prosopis juliflora* between 3.1-14.5 m, with an outlier reaching 18.1 m; *Hura crepitans* between 2.1-12.3 m; *Roystonea regia* between 3.7-12.7 m; *Albizia niopoides* between 4.4-17. 9 m; *Terminalia catappa* between 5.3-16.2 m; *Mangifera indica* between 3.8-13.2 m; *Samanea saman* between 3.7-23.7 m; *Melicoccus bijugatus* between 5.1 and 18.7 m; and *Delonix regia* between 4.6 and 12.5 m.

Diameter at breast height (DBH). The values for Tabebuia rosea are in a range of extremes between 11.7 - 57.3 cm; Enterolobium cyclocarpum between 10.8 - 140.1 cm with outliers up to 198.0 cm; *Azadirachta indica* between 12.4 - 36.4 cm; *Prosopis juliflora* between 12.4 - 98.7 cm, with an outlier of 114.6 cm; *Hura crepitans* between 11.1 - 60.5 cm; *Roystonea regia* between 19. 1-39.8 cm; *Albizia niopoides* between 14.6 - 85 cm; *Terminalia catappa* between 13.7-44.6 cm; *Mangifera indica* between 12.7 - 64.9 cm; *Samanea saman* between 11.5 - 108.9 cm, with an outlier value of 165.5 cm; *Melicoccus bijugatus* between 15.9 - 68.5 cm and *Delonix regia* between 15.5 - 97.1 cm, this for the 12 most representative species in the study area (Figure 5).

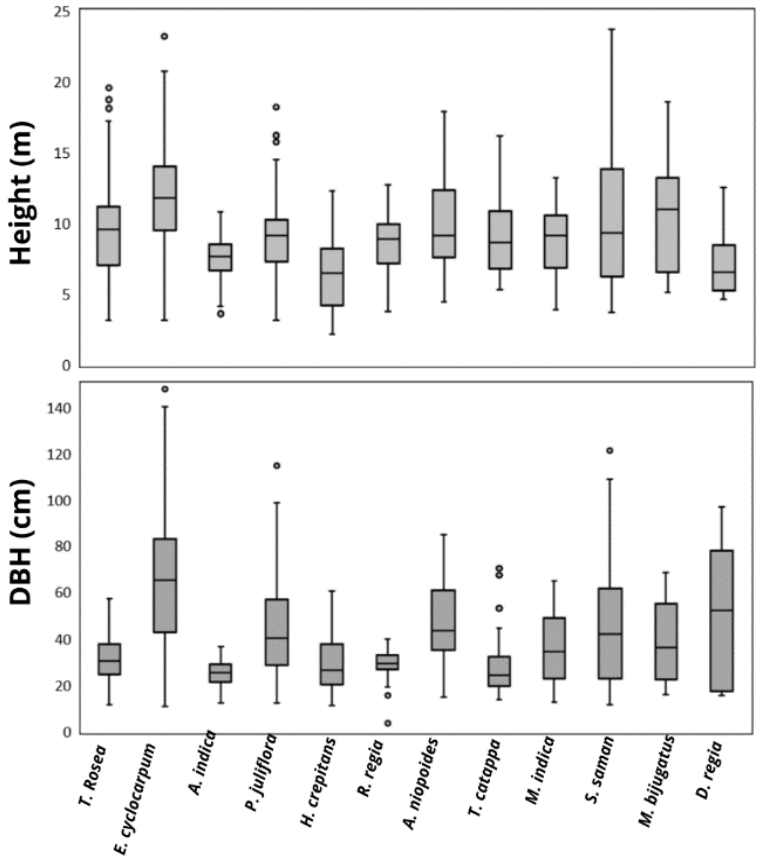

Figure 5. Box-and-whisker plot of total height (H) and diameter at breast height (DBH) in the 10 most representative species.

DBH – H Relationship. The scatter diagrams by species DBH-H (Figure 6) allowed the exploratory analysis of the data and served as support to interpret Pearson's correlation coefficient (r). The species with strong linear correlation (r ≥0.7) were: *Enterolobium cyclocarpum* (0.83), *Hura crepitans* (0.73), *Terminalia catappa* (0.85), *Mangifera indica* (0.7), and *Samanea saman* (0.91). *Tabebuia rosea* (0.56), *Prosopis juliflora* (0.68), *Albizia niopoides* (0.42), *Melicoccus bijugatus* (0.45), and *Delonix regia* (0.67) showed moderate linear correlation (0.4 ≤ r< 0.7), while *Azadirachta indica* (0.31) and *Roystonea regia* (0.26) exhibited weak linear correlation (r < 0.4).

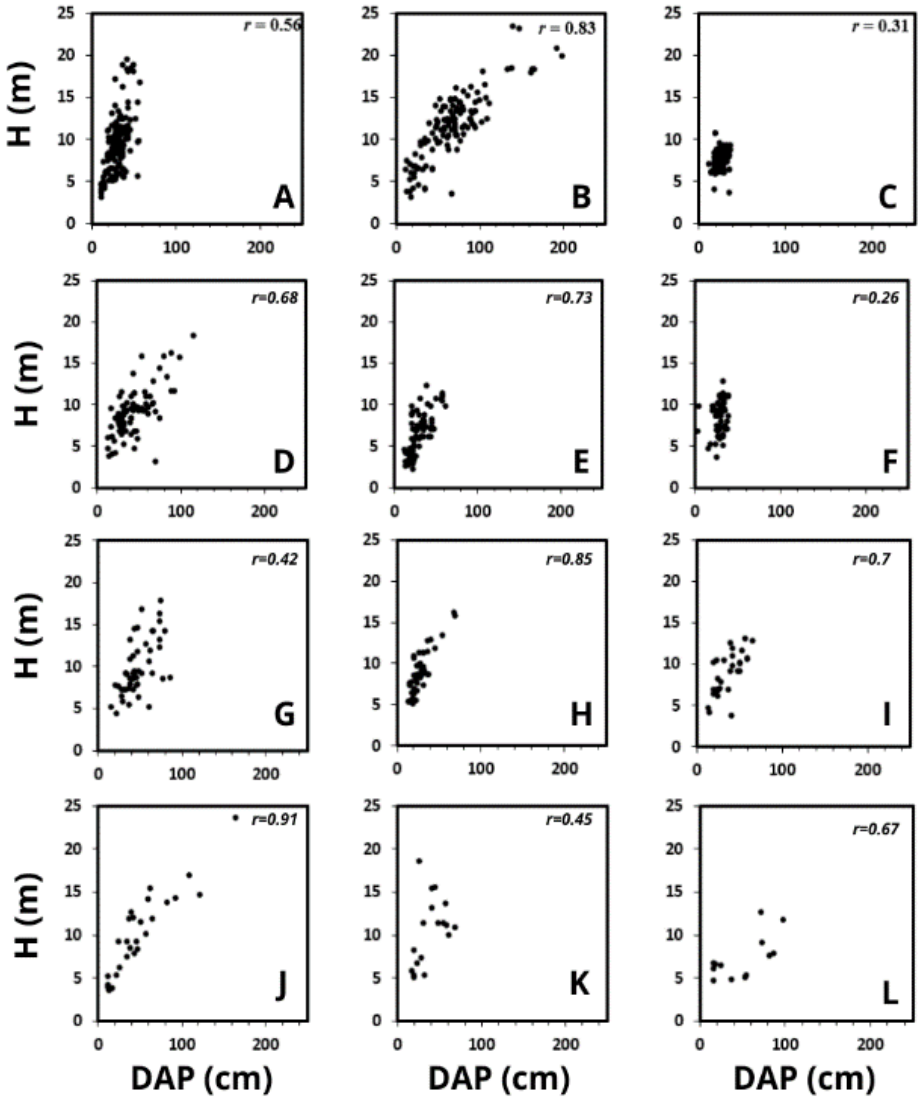

Figure 6. Scatter diagrams diameter at breast height (DBH)-total height (H) and Pearson's correlation coefficient (r). **A**) *Tabebuia rosea*; **B**) *Enterolobium cyclocarpum*; **C**) *Azadirachta indica*; **D**) *Prosopis juliflora*; **E**) *Hura crepitans*; **F**) *Roystonea regia*; **G**) *Albizia niopoides*; **H**) *Terminalia catappa*; **I**) *Mangifera indica*; **J**) *Samanea saman*; **K**) *Melicoccus bijugatus*; y **L**) *Delonix regia*.

Aerial biomass. The total aboveground biomass per species, estimated with the allometric equations a, b, c, d, and e (Table 4), from biometric measurements and stem density (Alvarez *et al*., 2012), is shown below expressed in tons of carbon (t C):

Table 4. Total aboveground biomass by species estimated with the allometric equations. a, b, c, d, and e.

Scientific name	Number of individuals	Density (g/cm^3)	Total aboveground biomass (t C)					
			a	***b***	***c***	***d***	***e***	**Mean**
Tabebuia rosea	146	0.54	3.21	3.61	5.35	3.72	0.69	3.32 ± 1.68
Enterolobium cyclocarpum	122	0.46	14.57	16.97	29.28	17.69	3.53	16.41 ± 9.18
Azadirachta indica	118	0.64	1.50	1.66	2.33	1.71	0.34	1.51 ± 0.72
Prosopis juliflora	83	0.67	4.64	5.33	8.64	5.53	1.17	5.06 ± 2.67
Hura crepitans	76	0.41	0.96	1.08	1.55	1.11	0.22	0.99 ± 0.48
Roystonea regia	62	0.71	1.26	1.41	2.04	1.45	0.29	1.29 ± 0.63
Albizia niopoides	50	0.55	2.54	2.89	4.57	3.00	0.60	2.72 ± 1.42
Terminalia catappa	44	0.48	0.78	0.88	1.31	0.91	0.16	0.81 ± 0.41
Mangifera indica	32	0.55	0.89	1.01	1.53	1.04	0.21	0.93 ± 0.47
Samanea saman	27	0.64	3.05	3.57	6.31	3.73	0.76	3.48 ± 1.98
Melicoccus bijugatus	18	0.87	1.00	1.14	1.81	1.18	0.24	1.07 ± 0.56
*Delonix regi*a	13	0.58	0.70	0.81	1.31	0.84	0.19	0.77 ± 0.40
Platymiscium pinnatum	8	0.68	0.24	0.28	0.44	0.29	0.24	0.26 ± 0.14
Ficus benjamina	7	0.46	0.19	0.21	0.32	0.22	0.19	0.20 ± 0.10
Crescentia cujete	6	0.58	0.11	0.12	0.18	0.12	0.11	0.11 ± 0.05
Bulnesia arborea	5	0.90	0.31	0.36	0.58	0.37	0.31	0.34 ± 0.18
Sterculia apetala	3	0.35	0.10	0.11	0.17	0.12	0.10	0.10 ± 0.05
Ceiba pentandra	3	0.29	0.02	0.02	0.04	0.03	0.02	0.02 ± 0.01
Cavanillesia platanifolia	2	0.32	0.09	0.10	0.15	0.10	0.09	0.09 ± 0.05
Bursera simaruba	2	0.32	0.01	0.01	0.02	0.01	0.01	0.011 ± 0.005
Guazuma ulmifolia	2	0.51	0.13	0.14	0.23	0.15	0.13	0.13 ± 0.07
Eriobotrya japonica	1	0.88	0.01	0.04	0.06	0.04	0.04	0.007 ± 0.003
Spondias mombin	1	0.4	0.04	0.21	0.32	0.22	0.19	0.04 ± 0.02

The total aerial biomass on the campus of the University of Magdalena, according to each allometric equation, is a = 36.35 t C, b = 41.7 t C, c = 68.23 t C, d = 43.35 t C, and e = 8.69 t C, whose average corresponds to 39.68 ± 21.24 t C, notoriously distancing from that reported by Srinivas & Sundarapandian (2019), who found biomass from 58 to 368 t C/ha. According to the five allometric equations, the average total aerial biomass per species indicates that the species with the highest aerial biomass content is *Enterolobium cyclocarpum*, which represents 41.35% of the total biomass on the campus, followed by *Prosopis juliflora* with 12.75%, *Samanea saman* with 12. 75%, *Tabebuia rosea* with 8.36%, *Albizia niopoides* with 6.86%, *Azadirachta indica* with

3.8%, *Roystonea regia* with 3.25%, *Melicoccus bijugatus* with 2.71%, *Hura crepitans* with 2.48%, *Mangifera indica* with 2.35%, *Terminalia catappa* with 2.04%, and *Delonix regia* with 1.94%. The other species listed represent less than 1% of the average total biomass, so the allometric equations recorded here can only be used and compared to determine the biomass of the same species in other regions with similar ecological conditions, as stated by Gómez *et al*. (2021), while differences in the magnitude of models c and e were detected for all species, while models a, b, and d show similar biomass magnitudes with a lag of fewer than 2 t.

Finally, the combined effects of photosynthetic efficiency, water status, and stress indicators, among others, determine plant productivity and diversity (Siyum, 2020; Stan & Sanchez-Azofeifa, 2019). Photosynthesis is thus a central metabolic pathway that integrates these variables; each factor influences and is influenced by the others. This research shows that water scarcity reduces photosynthetic capacity (NDVI < 0.3), creating a cycle that further stresses plants. The results suggest that management practices must prioritize the conservation and restoration of soil and its associated biodiversity to achieve optimal productivity in tropical dry forests, favor photosynthetic activity, and minimize stress-induced declines in productivity.

CONCLUSIONS

It is feasible to estimate the biomass of vegetation covers using differentiated indices, remote sensing, or remote sensing techniques, which reduce costs and time without having destructive implications on the vegetation. However, combining survey methods to characterize biomass structure and function in ecosystems is essential.

The range of NDVI variation in the study area was low (NDVI > 0.7 in 58% of the observations). The obtained fits between NDVI and precipitation are spatially acceptable. From a practical point of view, the relationship between precipitation and NDVI is linear between rainy seasons and the increase of vegetation indices in magnitude and extent.

The exercise allowed the development of a hybrid modeling approach (remote sensing and biophysical models) to consider different conditions associated with vegetation biomass in the Universidad del Magdalena's TDF and, with them, estimate and analyze changes that show the dynamics of vegetation cover of the permanent plot in a short period.

Enterolobium cyclocarpum represents the most significant contribution of above-ground biomass, which, according to models a, b, and d, is between 14.5 and 17.7 tons, followed by *Prosopis juliflora* with approximately five tons and *Tabebuia rosea* with three tons. *Azadirachta indica* and *Albizia niopoides* presented values close to two tons, and the other species showed values close to one ton.

ACKNOWLEDGMENTS

Thanks to the Vice-Rector's Office for Research at the Universidad del Magdalena and the graduate and undergraduate students and interns involved in the project.

Conflict of interest: The authors declare that there is no conflict of interest.

BIBLIOGRAPHIC REFERENCES

Aguirre, S.; Piraneque, N.; Mercado, T. (2022). *Suelo y cambio climático: Incluye estudio de casos.* 1a ed. Colombia: Editorial Unimagdalena. 196p.

Alvarez, E.; Duque, A.; Saldarriaga, J.; Cabrera, K.; de las Salas, G.; del Valle, I.; Lema, A.; Moreno, F.; Orrego, S.; Rodríguez, L. (2012). Tree above-ground biomass allometries for carbon stocks estimation in the natural forests of Colombia. *Forest Ecology and Management.* 267*:* 297-308. https://doi.org/10.1016/j.foreco.2011.12.013

Anaya-Acevedo, J. A.; Chuvieco Salinero, E.; Palacios Orueta, A. (2008). Estimación de biomasa aérea en Colombia a partir de imágenes MODIS. *Revista de Teledetección.* 30: 5-22.

Arrázola, P. G.; Buelvas, D. H.; Arrieta, D. Y. (2008). Aprovechamiento de las características nutricionales del almendro de la india (*Terminalia catappa* L.) como suplemento en la alimentación animal. *Revista MVZ Córdoba*. 13(1): 1205-1214.

Baseca, C. C. (2019). Plataforma tecnológica multimedia para la agricultura de precisión. https://riunet.upv.es/handle/10251/135820#

Becker-Reshef, I.; Justice, C.; Sullivan, M.; Vermote, E.; Tucker, C.; Anyamba, A.; Small, J.; Pak, E.; Masuoka, E.; Schmaltz, J.; Hansen, M.; Pittman, K.; Birkett, C.; Williams, D.; Reynolds, C.; Doorn, B. (2010). Monitoring Global Croplands with Coarse Resolution Earth Observations: The Global Agriculture Monitoring (GLAM) Project. *Remote Sensing*. 2(6): 6. https://doi.org/10.3390/rs2061589

Benítez, A.; Blanco-Torres, A.; Cabrera, M.; Calderón-Acevedo, C.; Castaño-Naranjo, A.; Castro-Lima, F.; Corzo, G.; Cuadros, H.; de Luna, G.; Devia, W.; Díaz-Pulido, A.; Etter, A.; Forero, F.; Galvis, G.; Gómez-Ruiz, D. A.; Gómez, J. P.; Gómez-Martínez, M.; González, F. A.; González, I., … Vergara-Valera, H. (2014). *El bosque seco tropical en Colombia.* Colombia: Instituto de Investigaciones de Recursos Biológicos Alexander von Humboldt. 350p.

Bernal, R.; Gradstein, S.; Celis, M. (Eds.). (2020). *Catálogo de plantas y líquenes de Colombia*. Colombia: Universidad Nacional de Colombia. 1504p.

Chave, J.; Riéra, B.; Dubois, M. A. (2001). Estimation of biomass in a neotropical forest of French Guiana: Spatial and temporal variability. *Journal of Tropical Ecology*. *17*(1): 79-96. https://doi.org/10.1017/S0266467401001055

Gautam, H.; Arulmalar, E.; Kulkarni, M. R.; Vidya, T. N. C. (2019). NDVI is not reliable as a surrogate of forage abundance for a large herbivore in tropical forest habitat. *Biotropica*. 51(3): 443-456. https://doi.org/10.1111/btp.12651

Girón-Angarita, K. J. (2021). Monitoreo del stock de carbono orgánico en suelos de ambientes subhúmedos. Estudio de caso departamento del Magdalena, Colombia. https://shorturl.at/1cdxs

Gómez, J. D.; Etchevers, J. D.; Campo, J.; Monterroso, A. I.; Paustian, K.; Asensio, C.; Gómez, J. D. (2021). Relaciones alométricas para estimar la biomasa aérea de especies tropicales de bosques estacionalmente secos del centro de México. *Madera y Bosques*. 27(4). https://doi.org/10.21829/myb.2021.2742441

Guzmán Q., J. A.; Sanchez-Azofeifa, G. A.; Espírito-Santo, M. M. (2019). MODIS and PROBA-V NDVI Products Differ when Compared with Observations from Phenological Towers at Four Tropical Dry Forests in the Americas. *Remote Sensing*. 11 (19): 2316. https://doi.org/10.3390/rs11192316

Gwal, S.; Singh, S.; Gupta, S.; Anand, S. (2020). Understanding forest biomass and net primary productivity in Himalayan ecosystem using geospatial approach. *Modeling Earth Systems and Environment*. 6(4): 2517-2534. https://doi.org/10.1007/s40808-020-00844-4

Hasnat, G. N.; Hossain, M. (2020). Global-Overview-of-Tropical-Dry-Forests. In: Bhadouria, R.; Tripathi, S.; Srivastava, P.; Singh, P. (eds.). *Handbook of Research on the Conservation and Restoration of Tropical Dry Forest.* pp. 1-23. 1 edition. U.S.A: IGI Global. 465p.

IDEAM. (2018). *Manual de Campo Inventario Forestal Nacional Colombia*. Bogotá, Colombia: Organización de las Naciones Unidas para la Alimentación y la Agricultura (FAO). 160p.

López, N.; Márquez Romance, A.; Guevara Pérez, E. (2020). Change dynamics of land-use and land-cover for tropical wetland management. *Water Practice & Technology*. 15(3): 632-644. https://doi.org/10.2166/wpt.2020.049

Mngadi, M.; Odindi, J.; Mutanga, O.; Sibanda, M. (2022). Estimating aboveground net primary productivity of reforested trees in an urban landscape using biophysical variables and remotely sensed data. *Science of The Total Environment.* 802: 149958. https://doi.org/10.1016/j.scitotenv.2021.149958

Mota, J. A. X.; Lemos, H. Á. F.; Ferreira, W. N.; Silva, M. A. M. (2020). Allelopathic effect of Azadirachta indica fresh leaves on the germination of native plants in the Seasonally Dry Tropical Forest. *Scientia Plena*. 16(12): 124202. https://doi.org/10.14808/sci.plena.2020.124202

Ochoa, C.; Patricia, L. (2020). Actividad insecticida de extractos de Azadirachta indica A. Juss. (Neemmeliaceae) sobre áfidos plagas en dos cultivos del género Vigna (Fabaceae) en el departamento de Córdoba (Colombia). https://shorturl.at/XAFZd

Paz Pellat, F.; Díaz-Solís, H. (2018). Relaciones entre la precipitación, producción de biomasa e índices espectrales de la vegetación: Alcances y limitaciones. *Terra Latinoamericana.* 36(2): 153-168. https://doi.org/10.28940/terra.v36i2.235

Phillips, J.; Duque, A.; Cabrera, K.; Yepes, A.; Navarrete, D.; García, M.; Álvarez, E.; Cabrera, E.; Cárdenas, D.; Galindo, G.; Ordoñez, M.; Rodríguez, M.; Vargas, D. (2011). *Estimación de las reservas potenciales de carbono almacenadas en la biomasa aérea en bosques naturales de Colombia*. Colombia: Instituto de Hidrología, Meteorología, y Estudios Ambientales (IDEAM). 68p.

Pluemjit, O.; Suksombut, W.; Kalpax, T.; Siriphanich, S. (2018). Flower development and factors affecting the blooming time of Tabebuia rosea (Bertol.) DC. *Acta Horticulturae*. 1201: 621-626. https://doi.org/10.17660/ActaHortic.2018.1201.83

R Core Team. (2022). R: Development Core Team, R: a language and environment for statistical computing. https://www.R-project.org

Rangel, J.; Cogollo, J.; Cortés-Duque, J.; Rivera Diaz, O. (2009). Amenazas a la biota (vegetación, fauna, flora, ecosistemas) de la Serranía del Perijá. In: Rangel, J.O. *Colombia, Diversidad Biótica VIII*. pp. 661-676. Colombia: Arfo Eds. 728p.

Revueltas, J. E.; Zabaleta, A.; Mercado, T.; Aguirre, S. (2020). Cambios en el clima local y su efecto en la regulación hídrica en microcuencas del departamento del Magdalena, Norte de Colombia. *Información tecnológica*. 31(6): 193-206. https://doi.org/10.4067/S0718-07642020000600193

Rouse Jr, J. W.; Haas, R. H.; Deering, D. W.; Schell, J. A.; Harlan, J.C. (1974). *Monitoring the vernal advancement and retrogradation (green wave effect) of natural vegetation.* EE.UU: Progress report NASA-CR-139243, Remote Sensing Center. College Station Texas. 8p.

Schlegel, B.; Gayoso, J.; Guerra, J. (2001). *Manual de procedimientos para inventarios de carbono en ecosistemas forestales.* Chile: Universidad Austral de Chile. 17p.

Sichaem, J.; Kaennakam, S.; Siripong, P.; Tip-pyang, S. (2012). Tabebuialdehydes A-C, cyclopentene dialdehyde derivatives from the roots of Tabebuia rosea. *Fitoterapia.* 83(8): 1456-1459. https://doi.org/10.1016/j.fitote.2012.08.010

Singh, B.; Jeganathan, C.; Rathore, V. S. (2020). Improved NDVI based proxy leaf-fall indicator to assess rainfall sensitivity of deciduousness in the central Indian forests through remote sensing. *Scientific Reports*. 10(1): 17638. https://doi.org/10.1038/s41598-020-74563-2

Siyum, Z. G. (2020). Tropical dry forest dynamics in the context of climate change: syntheses of drivers, gaps, and management perspectives. *Ecological Processes*. 9(1): 1-16. https://doi.org/10.1186/s13717-020-00229-6

Srinivas, K.; Sundarapandian, S. (2019). Biomass and carbon stocks of trees in tropical dry forest of East Godavari region, Andhra Pradesh, India. *Geology, Ecology, and Landscapes*. 3(2): 114-122. https://doi.org/10.1080/24749508.2018.1522837

Stan, K.; Sanchez-Azofeifa, A. (2019). Tropical dry forest diversity, climatic response, and resilience in a changing climate. *Forests*. 10(5): 443. https://doi.org/10.3390/f10050443

Thakur, T. K.; Swamy, S. L.; Bijalwan, A.; Dobriyal, M. J. R. (2019). Assessment of biomass and net primary productivity of a dry tropical forest using geospatial technology. *Journal of Forestry Research.* 30(1): 157-170. https://doi.org/10.1007/s11676-018-0607-8

Zaitunah, A.; Samsuri, Ahmad, A. G.; Safitri, R. A. (2018). Normalized difference vegetation index (ndvi) analysis for land cover types using landsat 8 oli in besitang watershed, Indonesia. *IOP Conference Series: Earth and Environmental Science.* 126*:* 012112. https://doi.org/10.1088/1755-1315/126/1/012112

